DEVELOPMENTAL BIOLOGY **195,** 1–15 (1998)
ARTICLE NO. DB978827

# *Hox* Group 3 Paralogs Regulate the Development and Migration of the Thymus, Thyroid, and Parathyroid Glands

**Nancy R. Manley[2] and Mario R. Capecchi[1]**

*Howard Hughes Medical Institute, Department of Human Genetics, University of Utah School of Medicine, Salt Lake City, Utah 84112-5331*

**The thymus, thyroid, and parathyroid glands in vertebrates develop from the pharyngeal region, with contributions both from pharyngeal endoderm and from neural crest cells in the pharyngeal arches. *Hoxa3* mutant homozygotes have defects in the development of all three organs. Roles for the *Hoxa3* paralogs, *Hoxb3* and *Hoxd3,* were investigated by examining various mutant combinations. The thyroid defects seen in *Hoxa3* single mutants are exacerbated in double mutants with either of its paralogs, although none of the double-mutant combinations resulted in thyroid agenesis. The results indicate that the primary role of these genes in thyroid development is their effect on the development and migration of the ultimobranchial bodies, which contribute the parafollicular or C-cells to the thyroid. *Hoxb3,Hoxd3* double mutants show no obvious defects in the thymus or parathyroids. However, the removal of one functional copy of *Hoxa3* from the *Hoxb3,Hoxd3* double mutants (*Hoxa3*$^{+/-}$,*Hoxb3*$^{-/-}$,*Hoxd3*$^{-/-}$) results in the failure of the thymus and parathyroid glands to migrate to their normal positions in the throat. Very little is known about the molecular mechanisms used to mediate the movement of tissues during development. These results indicate that *Hoxa3, Hoxb3,* and *Hoxd3* have highly overlapping functions in mediating the migration of pharyngeal organ primordia. In addition, *Hoxa3* has a unique function with respect to its paralogs in thymus, parathyroid, and thyroid development. This unique function may be conferred by the expression of *Hoxa3,* but not *Hoxb3* nor *Hoxd3,* in the pharyngeal pouch endoderm.** © 1998 Academic Press

## INTRODUCTION

The *Hox* gene family in the mouse consists of 39 genes encoding transcription factors which function to regulate embryonic development along the anteroposterior axis (Chisaka and Capecchi, 1991; Chisaka *et al.,* 1992; Le-Mouellic *et al.,* 1992; Condie and Capecchi, 1993, 1994; Dollé *et al.,* 1993; Gendron-Maguire *et al.,* 1993; Jeannotte *et al.,* 1993; Ramirez-Solis *et al.,* 1993; Rijli *et al.,* 1993, 1995; Small and Potter, 1993; Davis and Capecchi, 1994, 1996; Kostic and Capecchi, 1994; Davis *et al.,* 1995; Satokata *et al.,* 1995; Suemori *et al.,* 1995; Barrow and Capecchi, 1996; Benson *et al.,* 1996; Boulet and Capecchi, 1996; Fromental-Ramain *et al.,* 1996a,b; Goddard *et al.,* 1996; Zakany and Duboule, 1996). To date, the analysis of *Hox* genes has been primarily directed toward understanding their roles in the development of the somitic and neural crest-derived skeleton, the central nervous system, and the limbs. Much less is known about the roles these genes play in mediating organogenesis. Many of the *Hox* genes have complex expression patterns in developing organs, and even in adult organ tissue (Dony and Gruss, 1987; Gaunt, 1987; Krumlauf *et al.,* 1987; Fibi *et al.,* 1988; Holland *et al.,* 1988; Schughart *et al.,* 1988; Bogarad *et al.,* 1989; Gaunt *et al.,* 1989, 1990; Frohman *et al.,* 1990; Kress *et al.,* 1990; Dollé *et al.,* 1991; Whiting, 1991; Geada *et al.,* 1992; Sham *et al.,* 1992; Tan *et al.,* 1992; Wall *et al.,* 1992; Behringer *et al.,* 1993; Goto *et al.,* 1993; Haack and Gruss, 1993; Peterson *et al.,* 1994), but few of the *Hox* mutants described to date have been shown to have defects in organogenesis or organ function. This may indicate that the role of *Hox* genes in organogenesis is highly redundant. Consistent with this hypothesis, while neither *Hoxa11* nor *Hoxd11* single mutants show abnormal kidney development, *Hoxa11,Hoxd11* double mutants have severe kidney defects, including agenesis (Davis *et al.,* 1995).

The first *Hox* mutant mouse described, the *Hoxa3* mutant, has multiple defects in organogenesis. In addition to

[1] To whom correspondence should be addressed. Fax: (801) 585-3425/(801) 581-3770.

[2] Current address: Institute of Molecular Medicine and Genetics and Department of Pediatrics, Medical College of Georgia, Augusta GA 30912.

0012-1606/98 $25.00

defects in the development of the throat cartilages and cranial nerves (Chisaka and Capecchi, 1991; Manley and Capecchi, 1995, 1997), these mice mutant for *Hoxa3* showed deletions of the thymus, and parathyroids, as well as thyroid hypoplasia. *Hoxa3* is expressed in both the neural crest-derived mesenchymal cells of the pharyngeal arches and in the pharyngeal endoderm. The *Hoxa3* mutant phenotype appears to reflect deficiencies in both of these cell types (Manley and Capecchi, 1995).

The pharyngeal glandular organs in mammals have complex developmental origins. All of these organs, thyroid, thymus, parathyroids, and ultimobranchial bodies, develop concurrently and migrate from their sites of origin in the pharynx and pharyngeal pouches to their final positions along the ventral midline of the pharyngeal and upper thoracic region. The normal migration and development of these organs in the mouse is shown in Fig. 1. In addition to their migration patterns, the organ primordia interact with one another during these migrations. Although they arise independently, the parathyroids migrate in association with the thymic lobes and then stop and become closely associated with the thyroid gland. The parathyroids can become embedded within the thyroid, but always remain as a separate organ. Even more strikingly, the ultimobranchial bodies actually fuse with the thyroid in mammals, and their cells, the parafollicular cells, fully disperse with the thyroid follicular cells. This is in contrast to birds and fish, in which these complex movements and interactions do not take place. In chickens and zebrafish, the pharyngeal pouch-derived glands (thymus, parathyroids, and ultimobranchial bodies) develop entirely at their sites of origin and remain as bilateral pharyngeal structures. The molecular mechanisms underlying these movements in mammals are poorly understood. As we will see, however, it is intriguing that in mammals *Hox* genes, which are used to specify position along the major embryonic axis, also affect the migratory patterns of these organs.

Previously, we examined the effect of genetic interactions between mutations in group 3 paralogous *Hox* genes, *Hoxa3, Hoxb3,* and *Hoxd3,* on the formation of the axial skeleton and cranial ganglia (Manley and Capecchi, 1997). Surprisingly in the studies of cervical vertebrae formation, mice doubly mutant for *Hoxa3* and *Hoxd3* or *Hoxb3* and *Hoxd3* showed indistinguishable defects, the loss of the entire atlas. This result suggested that in the context of the first cervical vertebra, the identity of which specific *Hox* genes are functional within a region is not as critical as the total number of *Hox* genes operating in that region. Thus, the perspective changes from a qualitative one to a quantitative one. A molecular interpretation of this observation suggests that *Hox* genes may not be responsible individually for implementing a unique developmental program, but rather that multiple *Hox* genes may function together to mediate a program by controlling common target genes through common *cis* elements, and that for proper development, it is the stoichiometry of *Hox* genes operating within a developing tissue that is critical (Manley and Capecchi, 1997).

Nevertheless, particular *Hox* genes appear to have dominant roles in the development of specific structures. *Hoxd3,* for example, is more important than its paralogs in mediating the formation of the cervical vertebrae. While *Hoxd3*-mutant homozygotes show defects in the formation of the atlas and axis (Condie and Capecchi, 1993), *Hoxa3*-mutant homozygotes do not, and *Hoxb3* mutants show only very mild cervical vertebrae malformations at low penetrance (Manley and Capecchi, 1997). With respect to the formation of the pharyngeal glandular organs, *Hoxa3* appears to be the major player. As already mentioned, *Hoxa3*-mutant homozygotes have defects in the formation of the thymus, thyroid, and parathyroids. On the other hand, mice individually mutant for *Hoxb3* or *Hoxd3* do not show defects in these organs. We report here that there is also a quantitative component in the effect of *Hox3* genes on the development of the pharyngeal glandular organs. In mice doubly mutant for *Hoxa3* and *Hoxb3* or *Hoxa3* and *Hoxd3,* the defects in the thyroid and ultimobranchial bodies are exacerbated. Furthermore, while *Hoxb3,Hoxd3* double mutants have no obvious defects in the thymus or parathyroids, removal of one functional copy of *Hoxa3* from such double mutants ($Hoxa3^{+/-}$,$Hoxb3^{-/-}$,$Hoxd3^{-/-}$) results in the failure of these organ primordia to migrate to their normal positions in the throat. Thus, these three *Hox* genes have highly overlapping functions in mediating the proper migration of these organs.

## MATERIALS AND METHODS

### *Generation of Single, Double, and Triple Mutants and Genotype Analysis*

Mice heterozygous for the *Hoxa3, Hoxb3,* or *Hoxd3* mutation or homozygous for the *Hoxb3* mutation were intercrossed to generate homozygous mutants for each of the individual genes. Mouse colonies for the three double-mutant combinations were generated by crossing either *Hoxb3* heterozygous or homozygous mutants with *Hoxa3* or *Hoxd3* heterozygotes. The mutations in the *Hoxa3, Hoxb3,* and *Hoxd3* genes, and protocols for genotyping by Southern blot or PCR analysis, have been described previously (Chisaka and Capecchi, 1991; Condie and Capecchi, 1993; Manley and Capecchi, 1995, 1997). Double mutants were generated by intercrossing double heterozygous animals within each colony. Animals which were homozygous mutant for *Hoxb3* and heterozygous for either of the other paralogs were also used as parents in crosses to generate double mutants. $Hoxa3^{+/-}$,$Hoxb3^{-/-}$, $Hoxd3^{-/-}$ newborns were generated by intercrossing triple heterozygotes. All colonies were maintained on a mixed C57BL6 × 129Sv genetic background. Litters were collected for analysis immediately after birth, or at E18.5 by cesarean section. Embryonic age was estimated considering noon of the day of a vaginal plug as E0.5.

### *Histology*

For paraffin sectioning, newborn mice were sacrificed by $CO_2$ asphyxiation, fixed in 4% formaldehyde in phosphate-buffered saline (PBS), and embedded in Paraplast X-tra. Ten-micrometer sections were stained with hematoxylin and eosin (H&E), mounted in DPX, and photographed as previously described (Mansour *et al.,* 1993).

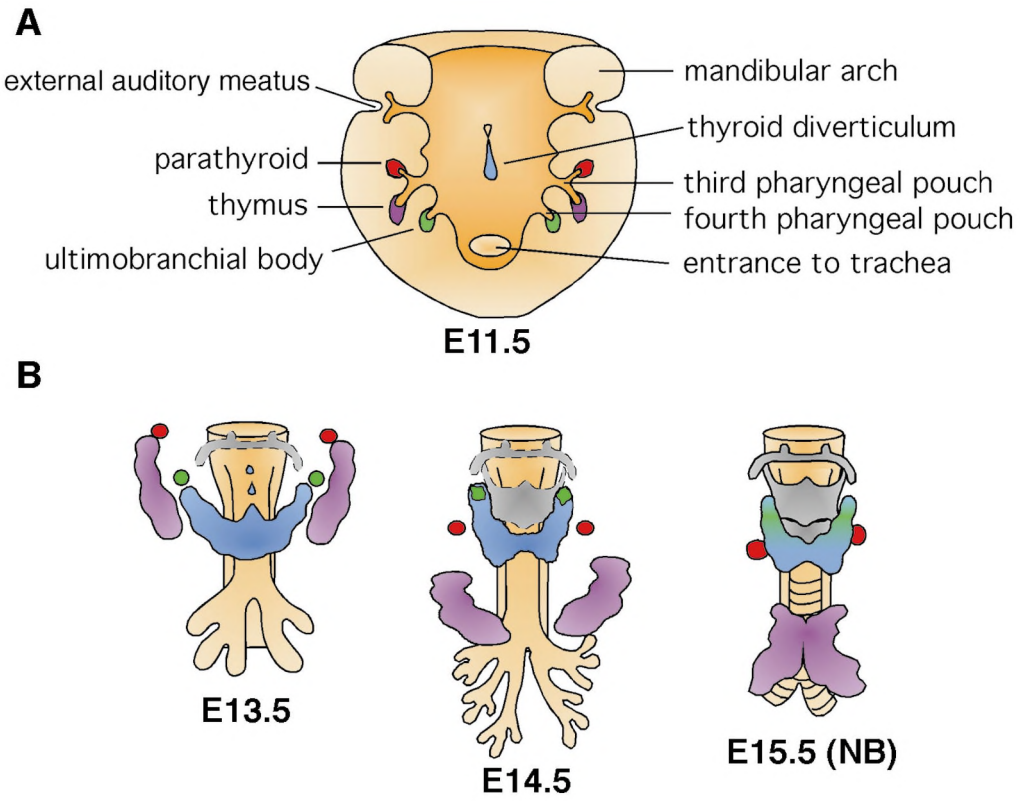


**FIG. 1.** Diagram of normal pharyngeal organ development in the mouse. (A) Dorsal view of the ventral half of the pharyngeal region of an E11.5-day embryo. The thyroid primordium forms first, at about E10.5, as a diverticulum from the ventral floor of the oropharynx, and is the source of thyroxin-producing follicular cells in the mature thyroid. By E11.5 the thyroid diverticulum, shown in blue, has separated from the floor of the pharynx at the approximate level of the second pharyngeal arch and is moving caudally down the ventral midline. The derivatives of the third and fourth pharyngeal pouches, the thymus, parathyroids, and ultimobranchial bodies are beginning to form. (B) By E13.5, the thyroid reaches its approximate final location and forms two lateral lobes connected caudally by an isthmus. Remnants of thyroid tissue along the medial migration route begin to disintegrate (blue dots). As the bilateral pouch-derived organ primordia form, they separate from the pharynx and migrate from their origination sites medially, ventrally, and caudally. The thymus and parathyroids migrate together. The two thymus primordia (purple) are lateral to the thyroid, and the parathyroids (red) are associated with the thymus lobes at their cranial ends. The ultimobranchial bodies (green) are near the cranial aspects of the thyroid lobes. The cartilage primordium of the hyoid bone begins to condense (gray). By E14.5, the thyroid has basically assumed its final shape, and is located ventral to the caudal aspect of the condensing laryngeal cartilages (gray). The ultimobranchial bodies are embedded in the thyroid lobes, but are still distinct structures. As they pass lateral to the thyroid lobes, the parathyroids detach from the thymus lobes and become associated with the thyroid. The parathyroids remain as separate organs, located lateral to or embedded in the thyroid lobes. The thymus lobes join at the midline and form a bilobed organ on the midline above the heart, in the anterior mediastinum. By E15.5 pharyngeal organ migration is essentially complete, although the ultimobranchial bodies are still visible as discrete cell populations within the thyroid lobes. They eventually fuse completely with the thyroid lobes, and in the newborn (NB) thyroid, ultimobranchial body-derived cells can be seen as calcitonin-positive cells distributed throughout the lobes (Hilfer, 1968; Rogers, 1927, 1971; Moseley *et al.*, 1968; Pearse and Carvalheira, 1967; Williams *et al.*, 1989).

### *Immunohistochemistry*

Calcitonin and thyroglobulin immunohistochemistry were performed as previously described (Manley and Capecchi, 1995). Both hormones were detected using commercially available polyclonal antibodies against human calcitonin or thyroglobulin (ICN). Appropriate staining was seen only in the thyroid or ultimobranchial bodies with both antibodies. Briefly, newborn animals were sacrificed by $CO_2$ asphyxiation, fixed in 4% formaldehyde in PBS overnight at room temperature, and embedded in paraffin. Ten- or 12-$\mu$m serial sections were collected and processed for immunostaining using a horseradish peroxidase-conjugated secondary antibody (Wall *et al.*, 1992; Gamer and Wright, 1993). Continuous serial sections from the level of the hyoid bone (or above) through the normal level of the thymus were examined. Primary antibody incubation was performed using a 1:200 dilution; appropriate secondary antibodies were used at 1:1000. Color reactions were developed using diaminobenzidine. Sections were counterstained with nuclear Fast Red (Mansour *et al.*, 1993), and mounted in DPX. Five each of the *Hoxa3,Hoxb3* and *Hoxb3,Hoxd3* double mutants were

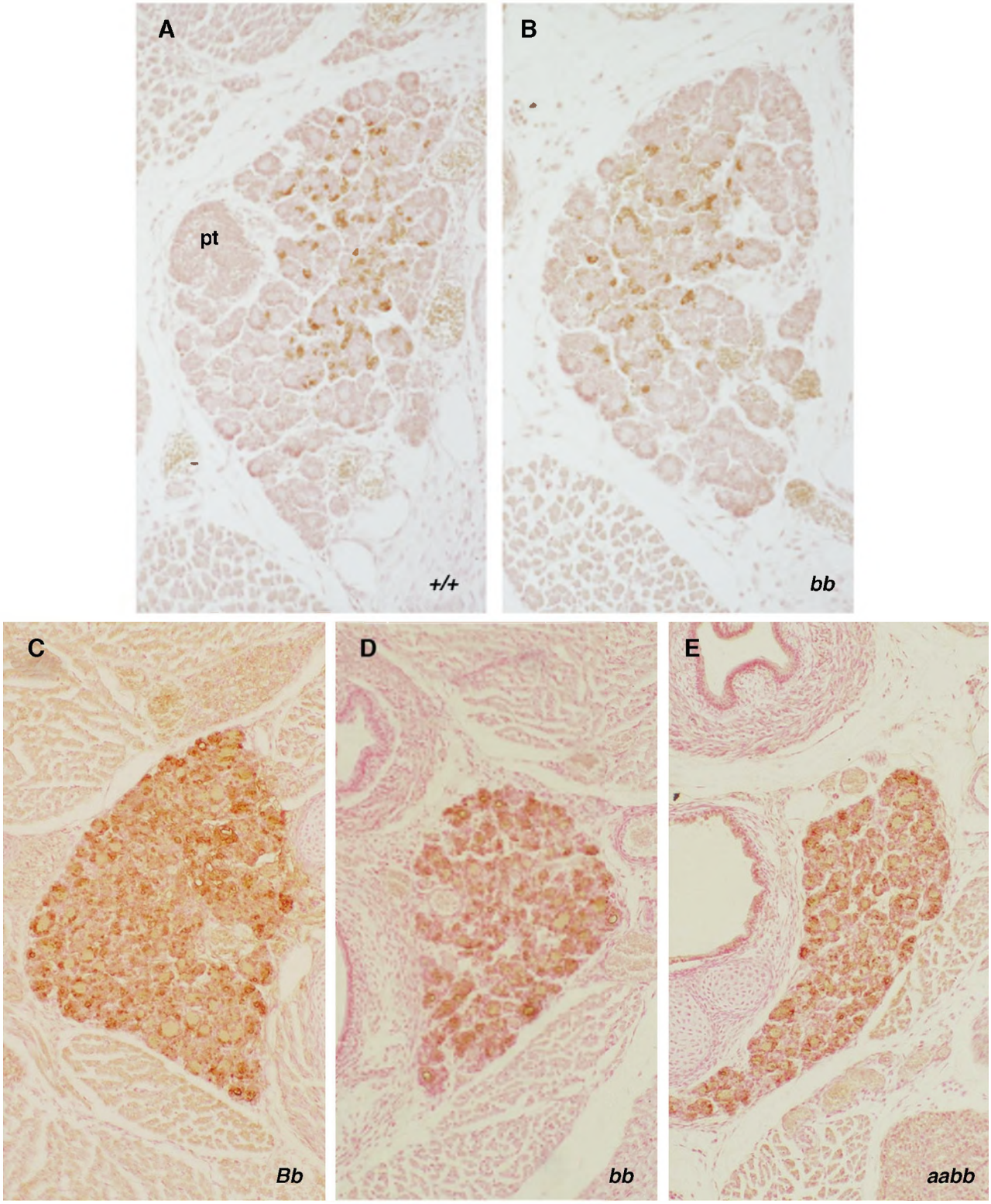


**FIG. 2.** Immunohistochemistry with anti-calcitonin (A and B) and anti-thyroglobulin (C–E) antibodies. Each panel shows a transverse section through one thyroid lobe of a newborn mouse. The signal was visualized with DAB (brown staining) and counterstained with nuclear Fast Red. Dorsal is up. (A) Calcitonin positive cells are scattered throughout the thyroid lobe in a wild-type animal. The parathyroid gland is also visible in this section (pt). (B) A similar pattern of staining is seen in a *Hoxb3* mutant newborn. (C–E) All genotype classes tested had the same pattern of staining with the anti-thyroglobulin antibody, with strong staining in the follicular cells and in the lumen of the follicles. +/+, wild type; *bb*, $Hoxb3^{-/-}$; *Bb*, $Hoxb3^{+/-}$; *aabb*, $Hoxa3^{-/-}$,$Hoxb3^{-/-}$.

**TABLE 1**
Summary of Thyroid and Ultimobranchial Body (ub) Defects

| | No. of ub defects | Types of ub defects present | Thyroid lateral lobe absent (hemiagenesis) | Thyroid isthmus defects present | Thymus phenotype | Parathyroid phenotype |
|---|---|---|---|---|---|---|
| *aa*[a] | 3/5 unilateral | 3 persistent | 3/5 | 3/5 absent<br>2/5 displaced | Absent | Absent |
| *bb* | 0/4 | — | 0 | 0 | Normal | Normal |
| *dd* | 0/5 | — | 0 | 0 | Normal | Normal |
| *aabb* | 2/5 unilateral | 1 persistent<br>1 absent[b] | 1/5 | 2/5 absent<br>3/5 pyramidal | Absent | Absent |
| | 3/5 bilateral | 1 persistent bilateral<br>1 persistent (L), partly fused (R)<br>1 persistent (L), absent (R) | | | | |
| *aadd* | 6/6 bilateral | persistent | 3/6 | 5/6 absent<br>1/6 pyramidal | Absent | Absent |
| *bbdd* | 2/5 bilateral | partly fused | 0 | 0 | Normal | Normal |
| *AaBbDd* | 0/5[c] | — | 0 | 0 | Normal | Normal |
| *AabbDd* | 2/2 unilateral | 2 persistent | 0 | 0 | 1 unilateral, ectopic | 1 bilateral, ectopic<br>1 unilateral, ectopic |
| *Aabbdd* | 0/2 | — | 0 | 0 | 2 bilateral, ectopic | 2 bilateral, ectopic |

[a] Genotype abbreviations are listed as: *aa, Hoxa3*$^{-/-}$*; bb, Hoxb3*$^{-/-}$*; dd, Hoxd3*$^{-/-}$. Multiple mutants are listed as combinations of these designations, i.e., *aabb, Hoxa3*$^{-/-}$*, Hoxb3*$^{-/-}$.

[b] Absent ubs were scored as absence of both a persistent ub and calcitonin-positive cells within the thyroid lobe on a single side; see text.

[c] None of the three mutant classes containing all three genes (*AaBbDd, AabbDd, Aabbdd*) were assayed for calcitonin expression; therefore, ub phenotypes were scored only for persistent, but not absent or partly fused, ubs.

examined by immunohistochemistry with both antibodies. Six *Hoxa3,Hoxd3* mutants were examined, three with antibody staining and three with H&E staining of serial sections.

### *Whole-Mount in Situ Hybridization and Sectioning*

Whole-mount *in situ* hybridizations were performed as described (Carpenter *et al.*, 1993; Manley and Capecchi, 1995). E10.5 mouse embryos were fixed overnight in 4% formaldehyde in PBS, then dehydrated into methanol and stored at −20°C until use. The digoxigenin-labeled RNA probes were used at 0.5 μg/ml. Alkaline phosphatase-conjugated anti-digoxigenin Fab fragments were used at 1:5000. Color reactions were carried out for 2 to 15 h. Embryos were photographed without clearing with Ektachrome 160T film using a Wild dissecting microscope.

The following probes were used for whole-mount *in situ* hybridization. The *Hoxa3* antisense probe was transcribed from a 650-base-pair *Eco*RI cDNA fragment containing part of the first coding exon and the homeobox (Manley and Capecchi, 1995). The *Hoxb3* probe was made from a 550-bp cDNA fragment which spans the *Hoxb3* stop codon and included part of the 3′UTR. The *Hoxd3* probe was made from a 900-bp cDNA fragment which has been previously described (Condie and Capecchi, 1993).

Embryos stained in whole mount were processed for sectioning by standard paraffin embedding. Embryos were sectioned at 10 μm, counterstained with nuclear Fast Red (Mansour *et al.*, 1993), and mounted in DPX. Sections were photographed in bright field with didymium and neutral density filters using Ektachrome 64T film on a Leitz Ortholux microscope.

## RESULTS

### *Hoxb3 and Hoxd3 Single Mutants Have Normal Thyroid Glands*

The generation and characterization of mice with individual targeted disruptions in *Hoxa3, Hoxb3,* or *Hoxd3* have been previously described (Chisaka and Capecchi, 1991; Condie and Capecchi, 1993; Manley and Capecchi, 1997). The thyroid defects in *Hoxa3* single mutants include hemiagenesis of the thyroid, deletion or displacement of the isthmus, and reduction or absence of C cells in the thyroid lobes (Manley and Capecchi, 1995). Lack of C cells in the thyroid in these mutants is associated with the failure of the ultimobranchial bodies, containing the C cells, to fuse with the thyroid. Both *Hoxb3*$^{-/-}$ and *Hoxd3*$^{-/-}$ animals have a thyroid gland that appears normal in size and organization. These mutant animals showed a bilobed thyroid with well-organized follicles and a normally placed isthmus that were indistinguishable from wild type.

For a more detailed analysis of the thyroid, immunohistochemistry was performed using antibodies raised against calcitonin and thyroglobulin. Calcitonin is made by the C cells, which originate in the ultimobranchial body. Thyroglobulin is made and secreted by the follicular cells, and should be present both in the follicular cells and in the lumen of the follicles. Both of these markers showed normal

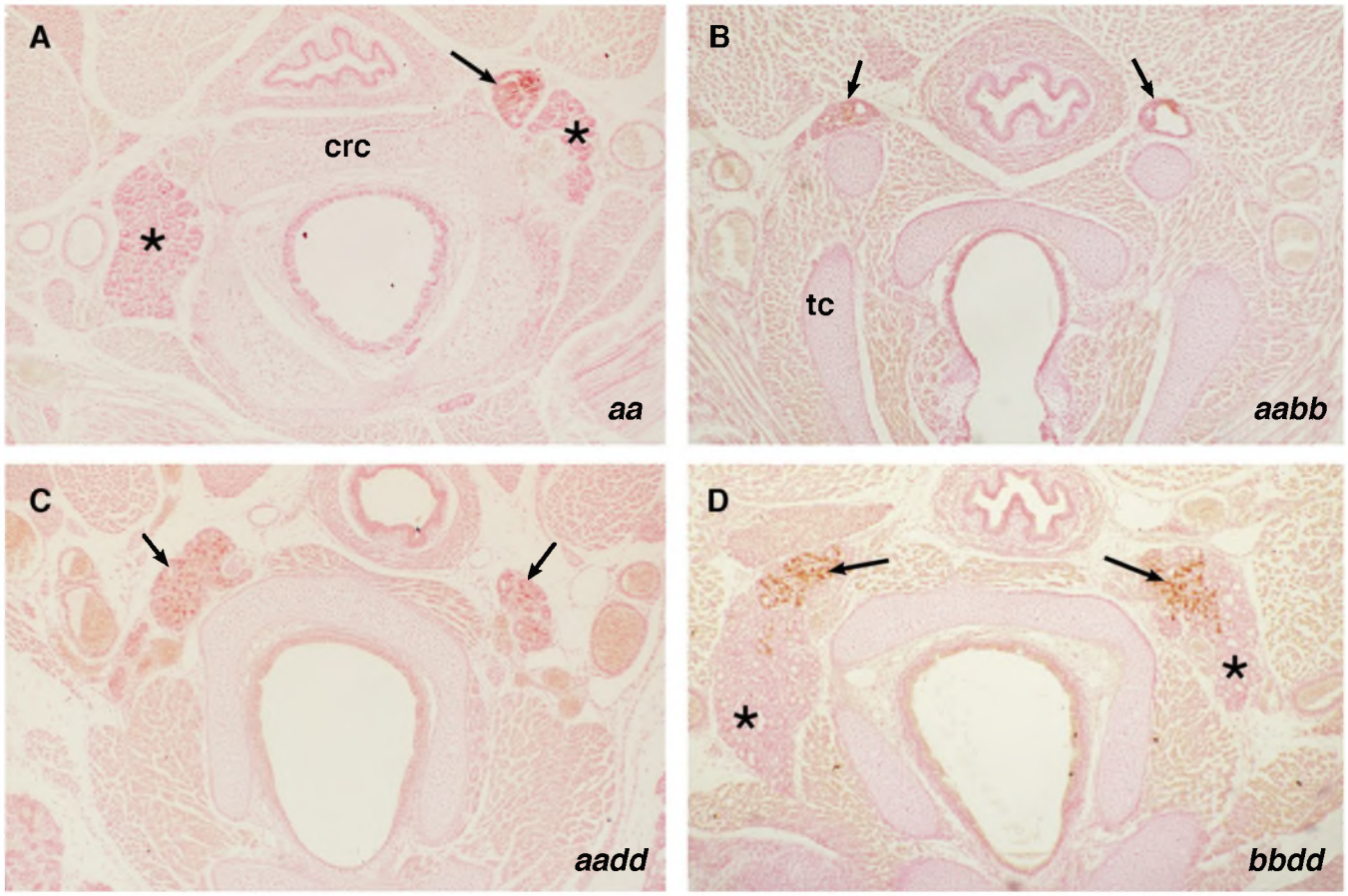


**FIG. 3.** Bilateral ultimobranchial body phenotypes in the double mutants. Transverse sections through newborns, stained with anti-calcitonin antibody (brown staining). Arrows point to persistent (A), ectopic (B and C), or partially fused (D) ultimobranchial bodies. Asterisks indicate thyroid lobes. Dorsal is up. (A) A *Hoxa3* mutant (*aa*) with a unilateral persistent ultimobranchial body at the dorsal and anterior end of one thyroid lobe, at the level of the cricoid cartilage (crc). (B) A $Hoxa3^{-/-}$,$Hoxb3^{-/-}$ double mutant (*aabb*), with bilateral ectopic ultimobranchial bodies, located dorsal to the anterior end of the thyroid cartilage (tc), and far anterior to the thyroid lobes. (C) A $Hoxa3^{-/-}$,$Hoxd3^{-/-}$ double mutant (*aadd*), with bilateral ectopic ultimobranchial bodies. Both ultimobranchial bodies contain follicular structures, but are clearly separated from and located anterior to the thyroid lobes (at the levels of the cricoid cartilage). (D) A $Hoxb3^{-/-}$,$Hoxd3^{-/-}$ double mutant (*bbdd*) with bilateral partially fused ultimobranchial bodies at the dorsal and anterior ends of the thyroid lobes.

distribution and cellular localization in the $Hoxb3^{-/-}$ and $Hoxd3^{-/-}$ newborn thyroid glands, indicating that there was no apparent defect in thyroid development in these mutants (Fig. 2 and data not shown). Calcitonin-positive cells were present in normal numbers and were distributed throughout both thyroid lobes. Both the follicular cells and the colloid in the thyroid follicles were strongly positive for thyroglobulin. Analysis of the *Hoxa3* single mutant with the thyroglobulin antibody also showed strong production and secretion of thyroglobulin, even in animals which showed disorganization of the thyroid follicles (not shown). These results show that only the *Hoxa3* single mutants have defects in the thyroid and ultimobranchial bodies, and that none of the mutations individually affects the ability of the follicular cells to produce and secrete thyroglobulin.

### *Both Hoxb3 and Hoxd3 Mutations Exacerbate the Hoxa3 Ultimobranchial Body Mutant Phenotype*

In order to determine whether *Hoxb3* and *Hoxd3* contribute to the formation of the thyroid, all three double mutants were examined at the newborn stage for both calcitonin and thyroglobulin expression. The results were then compared to those obtained with the *Hoxa3* mutants, and are summarized in Table 1. Exacerbation of the $Hoxa3^{-/-}$ ultimobranchial body phenotype was seen in both the *Hoxa3,-Hoxb3* and the *Hoxa3,Hoxd3* double mutants. None of the double-mutant combinations resulted in thyroid agenesis.

In the previous analysis of *Hoxa3* single mutants, unilateral persistent ultimobranchial bodies (i.e., ones not fused with the thyroid as is normal) were seen in three of five mutants examined. The remaining two *Hoxa3* mutants had

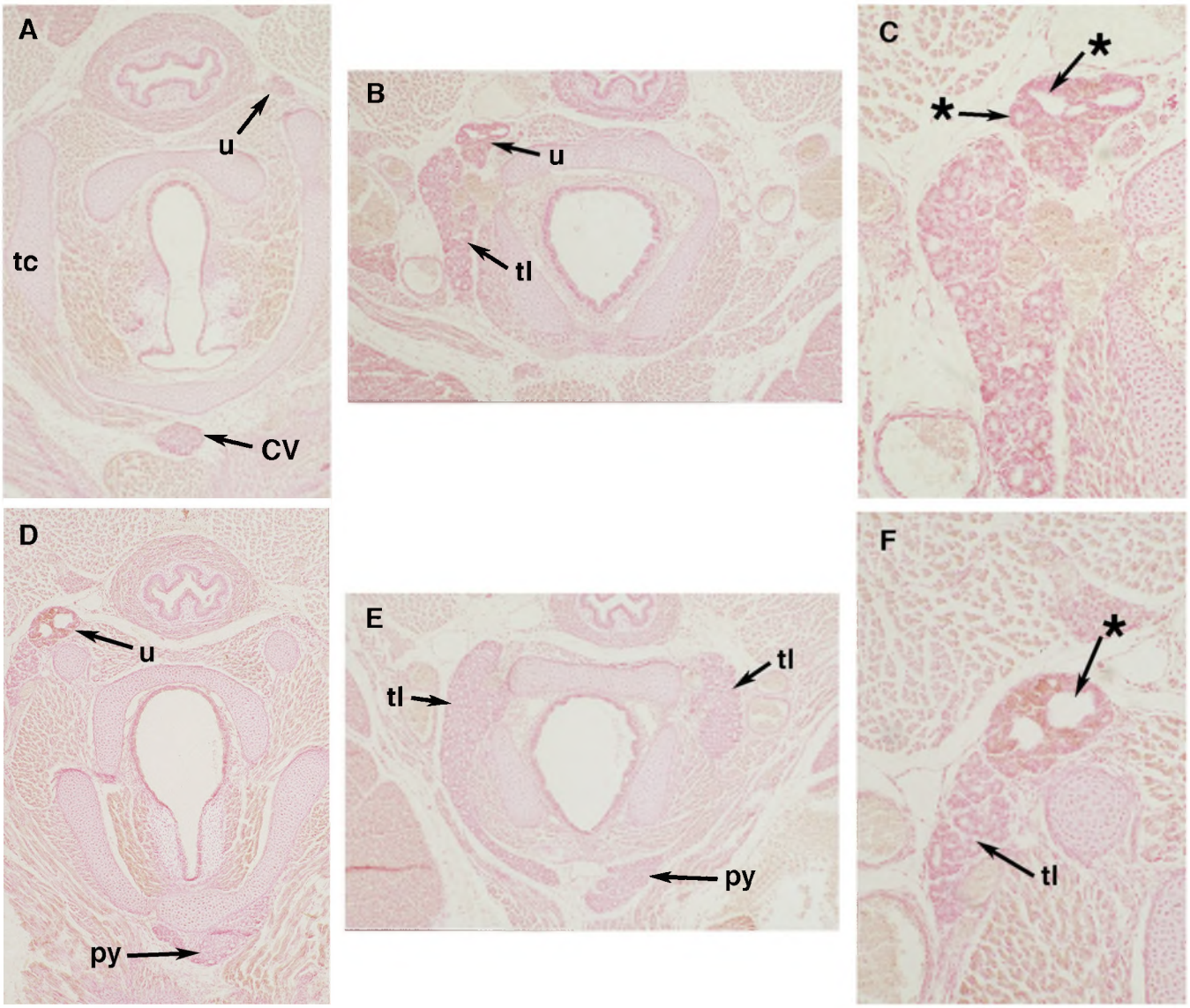


**FIG. 4.** Thyroid lobe and ultimobranchial body defects in *Hoxa3,Hoxd3* (A–C) and *Hoxa3,Hoxb3* (D–F) double mutants. Transverse sections through newborns, stained with anti-calcitonin antibody (brown staining). (A) Section showing an ectopic ultimobranchial body (u) and cervical thyroid tissue (cv) present at the anterior part of the thyroid cartilage (tc). (B) More posteriorly in the same animal, a single thyroid lobe (tl) is present at its normal location, with an associated persistent ultimobranchial body. No isthmus or right thyroid lobe was present in this animal. (C) Higher magnification of the thyroid lobe and persistent ultimobranchial body in B. The ultimobranchial body is lightly stained for calcitonin, and contains follicle-like structures (asterisks). (D) A *Hoxa3,Hoxb3* animal with a single persistent ultimobranchial body and a pyramidal thyroid lobe (py), that reached more anteriorly than the lateral thyroid lobes. (E) Both lateral lobes and the pyramidal lobe seen at a more posterior section. These three lobes remained as separate lobes, not fusing at any axial level. Because no calcitonin-positive cells were ever present on the right side of this animal, it was scored as having one persistent and one absent ultimobranchial body. (F) Higher magnification of the section shown in D, showing the calcitonin-positive ultimobranchial body and the adjacent anterior end of the left thyroid lobe. This ultimobranchial body has holes that do not have a follicular appearance (asterisk). cv, cervical thyroid tissue; py, pyramidal thyroid lobe; tc, thyroid cartilage; tl, thyroid lobe; u, ultimobranchial body.

normal numbers and distribution of C cells within the thyroid. Both *Hoxa3,Hoxb3* and *Hoxa3,Hoxd3* double mutants had a 100% penetrance of persistent ultimobranchial bodies. In addition, three of five *Hoxa3,Hoxb3* and all *Hoxa3,-Hoxd3* double mutants had a bilateral ultimobranchial body phenotype, which was never seen in the *Hoxa3* single mutants.

In the *Hoxa3,Hoxd3* double mutants, all animals showed bilateral persistent ultimobranchial bodies, located anterior and dorsal to the thyroid lobes (Figs. 3B and 3C). In the

*Hoxa3,Hoxb3* double mutants, a variety of ultimobranchial body phenotypes was seen, including absent, persistent, and partially fused ultimobranchial bodies. Both bilateral and unilateral defects were seen, and phenotypes often differed on two sides of the same animal (Fig. 4). Absence of ultimobranchial bodies was scored as those cases exhibiting no persistent ultimobranchial body and no C cells in the thyroid lobe. Cases scored as partially fused ultimobranchial bodies were those in which a group of calcitonin-producing cells was attached to the dorsal anterior end of one follicular lobe, but the cells had not integrated into the thyroid follicular structure.

The *Hoxb3,Hoxd3* double mutants also showed partially fused ultimobranchial bodies, although at low penetrance. Of five newborns examined, two showed partially fused ultimobranchial bodies, one bilaterally (Fig. 3D), and one unilaterally. The remaining animals showed normal numbers and distribution of C cells within the thyroid lobes. Partially fused ultimobranchial bodies were not seen in the six wild-type, four $Hoxb3^{-/-}$, and five $Hoxd3^{-/-}$ animals examined.

An additional feature of the persistent ultimobranchial bodies seen in the double mutants is that they were consistently located more anteriorly in these animals than those seen in the *Hoxa3* single mutants. Persistent ultimobranchial bodies in *Hoxa3* single mutants were located adjacent to the anterior end of the thyroid lobes, at the posterior aspect of the thyroid cartilage. Persistent ultimobranchial bodies in the double mutants were often located at the most dorsal and anterior aspect of the thyroid cartilage (Figs. 3B, 4A, and 4D), 50–100 $\mu$m anterior to the thyroid lobes. The ectopic location of these persistent ultimobranchial bodies suggests a separate defect in organ migration, as opposed to the failure of the ultimobranchial bodies to fuse with the thyroid lobes as seen in the *Hoxa3* mutants (see below).

Some ultimobranchial bodies also contained what appeared to be follicular structures (Figs. 3C and 4C), or large holes (Figs. 3B and 4F). Examination of the ultimobranchial bodies present in H&E-stained sections of *Hoxa3,Hoxd3* double mutants showed that these follicular structures did contain colloid, which indicates the production and secretion of thyroglobulin (data not shown). In the *Hoxa3,Hoxd3* double mutant shown in Fig 3C, both ultimobranchial bodies have numerous follicles; however, these ultimobranchial bodies are far anterior to and well separated from the thyroid lateral lobes, and there are no calcitonin positive cells present in the thyroid lobes themselves. We interpret these to indeed be ectopic ultimobranchial bodies, rather than fragments of the thyroid lobes. These results support the possibility that follicular cells can arise from ultimobranchial bodies as well as from the thyroid diverticulum (see Discussion).

### *Structure of the Thyroid Lobes in Double Mutants*

Double mutants were also scored for defects in the structure of the thyroid gland itself, to determine if all three genes also had a role in the development of the thyroid diverticulum. The thyroid normally consists of two lateral lobes, joined at the caudal end by an isthmus of follicular tissue located ventral to the trachea (see Fig. 1). Both the *Hoxa3,Hoxb3* and *Hoxa3,Hoxd3* double mutants had a 100% penetrance of defects in the isthmus, and penetrance of defects in lateral lobe structure similar to that of the *Hoxa3* single mutant (Table 1). Although the penetrance was similar, the severity of these defects did increase in these double mutants, particularly in the isthmus. In the *Hoxa3,Hoxd3* double mutants, five of six animals had no isthmus, increased from three of five in the *Hoxa3* single mutant (Table 1). One of these animals also had small remnants of cervical thyroid tissue far cranial to the thyroid lobes (Fig. 4A). In the one remaining *Hoxa3,Hoxd3* double mutant, and in the three cases where thyroid tissue was present in the ventral midline in the *Hoxa3,Hoxb3* double mutants, it appeared as a pyramidal lobe (triangular thyroid lobe extending anteriorly from the isthmus in the ventral midline), rather than a simple anterior displacement of the isthmus (Figs. 4D and 4E; Table 1). In both of these double-mutant classes, this pyramidal lobe attached either to only one lateral lobe or to neither lobe (Fig. 4E). In the *Hoxa3* single mutants with a displaced isthmus, the morphology was normal, not pyramidal (not shown). Although the apparent increase in the frequency of isthmus deletion in the *Hoxa3,Hoxd3* double mutants is not statistically significant due to the small numbers of animals examined, this observation combined with the morphology of the ventral thyroid tissue when present in these double mutants supports

**FIG. 5.** Ectopic thymus in $Hoxa3^{+/-}$,$Hoxb3^{-/-}$,$Hoxd3^{-/-}$ mice. Transverse H&E-stained sections of newborn mice. (A) The thymus (th) in a wild-type mouse is a large bilobed organ located in the anterior mediastinum, between the left and right superior vena cavae (vc) and ventral to the aorta (ao). (B) The thymus of a $Hoxb3^{-/-}$,$Hoxd3^{-/-}$ double mutant (*bbdd*) appears normal. (C) No thymus tissue is present in the normal position of the thymus in a $Hoxa3^{+/-}$,$Hoxb3^{-/-}$,$Hoxd3^{-/-}$ mouse (*Aabbdd*). (D) Bilateral thymus lobes are present ectopically, here seen at the level of the arytenoid cartilages in the larynx (ar). ao, aorta; ar, aratynoid cartilages; th, thymus; vc, superior vena cava.

**FIG. 6.** Ectopic parathyroid glands in multiple mutants. Transverse H&E-stained sections of newborn mice. (A) Normally placed parathyroid gland (pt) embedded in the thyroid lobe (tl) of a triple heterozygote (*AaBbDd*). (B). Ectopic parathyroid (pt) and thymus lobe (th) in a $Hoxa3^{+/-}$,$Hoxb3^{-/-}$,$Hoxd3^{+/-}$ newborn (*AabbDd*). The parathyroid is located next to the external carotid artery (ec). (C) Similar view of an ectopic parathyroid and thymus in a $Hoxa3^{+/-}$,$Hoxb3^{-/-}$,$Hoxd3^{-/-}$ newborn (*Aabbdd*). (D) Lower magnification of the same section shown in C, showing the bilateral parathyroids medial to the cochlea (co). At this level the nasopharynx and the oropharynx (np and op) are still separate. The ectopic parathyroids in B and C have a characteristic appearance of densely packed small cells with dark nuclei and pink cytoplasm; compare with the parathyroid in A, shown at the same magnification. co, cochlea; ec, external carotid artery; np, nasopharynx; op, oropharynx; pt, parathyroid; th, thymus.

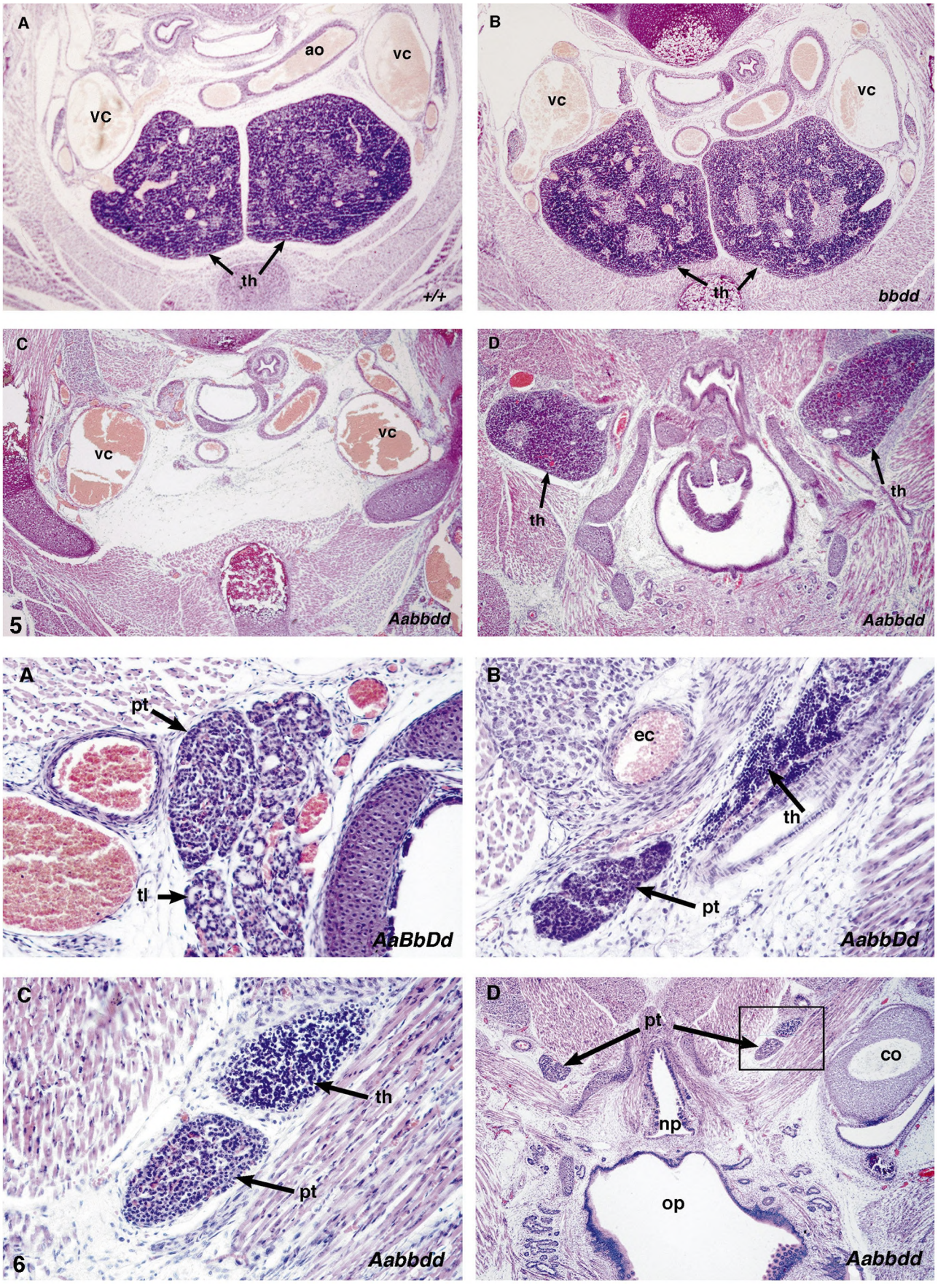
A
ao
vc
VC
th
+/+
B
vc
vc
th
bbdd
C
vc
vc
5
Aabbdd
D
th
th
Aabbdd
A
pt
tl
AaBbDd
B
ec
th
pt
AabbDd
C
th
pt
6
Aabbdd
D
pt
co
np
op
Aabbdd

the conclusion that thyroid defects are increased. The *Hoxb3,Hoxd3* double mutants examined showed no defects in the structure of the thyroid lobes or the isthmus.

All single and double mutants were also tested for thyroglobulin production by immunohistochemistry. All mutant classes showed strong immunoreactivity to the thyroglobulin antisera in both the follicular cells and the colloid of the follicles, indicating normal expression of thyroglobulin (Fig. 2E and data not shown).

### *Group 3 Paralogs Regulate the Migration of the Thymus and Parathyroids*

Because the *Hoxa3* mutant has an early deletion of the thymus and parathyroids, double mutants with *Hoxa3* were not informative as to the role of the other paralogs in the development of these organs. Previous histological examination of *Hoxd3* single mutants showed no obvious defects in the thymus and parathyroids (Condie and Capecchi, 1993). We also saw no defect in the thymus or parathyroids in the *Hoxa3* heterozygous, *Hoxb3* single-mutant, or *Hoxb3,Hoxd3* double-mutant newborns. The thymus was of normal size and placement, and had well-organized cortex and medullary regions (Fig. 5B; Table 1). Parathyroids were always present bilaterally near the thyroid, and appeared normal (data not shown).

Because mutations in *Hoxa3* alone have such a profound impact on thymus development, any functions of the *Hoxb3* and *Hoxd3* genes would be masked in mice with two mutant copies of the *Hoxa3* gene. Therefore, we serially sectioned two newborn mice with only a single wild-type copy of *Hoxa3* and mutant copies of all other genes within this paralogous group (i.e., $Hoxa3^{+/-}$, $Hoxb3^{-/-}$, and $Hoxd3^{-/-}$ mice). In both of these animals, the thymus was formed, but appeared as two lateral lobes displaced anteriorly from the normal location of the thymus (Table 1; Figs. 5C and 5D). The organization and overall size of these lobes were similar to wild type, with clearly recognizable cortical and medullary regions. These ectopic lobes extended from a position medial to the cochlea posteriorly to the level of the thyroid gland. Ectopic parathyroid glands were found adjacent to the anterior ends of these ectopic thymus lobes (Table 1; Figs. 6C and 6D). The thyroid itself appeared relatively normal, with normal location, lobe structure, and isthmus (recall that the $Hoxb3^{-/-}$,$Hoxd3^{-/-}$ newborns had grossly normal thyroid structure). No ectopic ultimobranchial bodies were identified; however, due to the low frequency at which animals of this genotype were obtained, immunohistochemistry for calcitonin was not performed, so the absent or partially fused ultimobranchial mutant phenotype could not be scored. A diagram of the ectopic position of the thymus and parathyroids in these mutant mice is shown in Fig. 7.

The degree of overlap that these genes have for this function was further defined by the analysis of other genotypes that combine mutations of all three paralogs. All five triple heterozygotes examined had normal thymus, parathyroid, and thyroid glands as shown by H&E staining of sectioned material (Table 1; Fig. 6A). Removal of one additional copy of *Hoxb3* ($Hoxa3^{+/-}$,$Hoxb3^{-/-}$,$Hoxd3^{+/-}$), resulted in a unilateral ectopic thymus, bilateral ectopic parathyroids, and one ectopic ultimobranchial body in one of two animals examined with this genotype (Figs. 5A and 5C and data not shown). The other half of the thymus in this animal was located at the midline, similar to the normal position for the thymus. The second animal of this genotype had normal thymus and thyroid glands, but still had one ectopic parathyroid gland and one ectopic ultimobranchial body. The combination of defects seen in these animals shows that parathyroid and thymus migration can be affected separately, even though they normally migrate together. None of the five $Hoxb3^{-/-}$,$Hoxd3^{-/-}$ double mutants examined ever showed ectopic organs, indicating that at least one copy of all three paralogs must be mutated in order to see this mutant phenotype. The normal appearance of the triple heterozygotes further suggests that this phenotype requires the mutation of at least four total copies of the group 3 paralogs, indicating that this is a highly redundant function of this gene family.

### *Only Hoxa3 Is Expressed in the Pharyngeal Pouch Endoderm*

The results from the analysis of $Hoxa3^{+/-}$,$Hoxb3^{-/-}$, $Hoxd3^{-/-}$ newborns show that while the migration of the thymus, the ultimobranchial bodies, and parathyroids is redundantly specified, the development of the thymus and parathyroids requires at least one functional copy of the *Hoxa3* gene to occur normally. Therefore, the formation of the thymus and parathyroids appears to be one function of these paralogous genes that is not redundantly specified. This result could reflect a difference in the function of these closely related genes, a difference in their expression patterns, or both. At E9.5, these genes have been reported to have similar expression patterns in the hindbrain, neural crest, and pharyngeal arches (Hunt *et al.,* 1991a,b). We examined the expression patterns of these three genes in the pharyngeal region at E10.5, immediately prior to the onset of pharyngeal organogenesis (Cordier and Haumond, 1980). Wild-type embryos were stained in whole mount for each of the three genes, and then sectioned to determine the cellular localization of the signal.

At this stage of development, the expression patterns of the three genes are similar, but not identical. All three genes are extensively coexpressed in the mesenchyme of the fourth and sixth arches, which is primarily neural crest-derived (Fig. 8). In the third arch, *Hoxd3* is expressed in only a small subset of dorsally located cells, and *Hoxb3* seems to be primarily expressed in more lateral regions of the third arch mesenchyme. *Hoxa3* is strongly expressed throughout the mesenchymal cells of the third arch. Most strikingly, *Hoxa3* is the only one of these paralogs to be expressed in the endodermal cells of the third and fourth pouch (Figs. 8A and 8D). This unique expression of *Hoxa3* in the pouch endoderm could provide an explanation for the apparently unique function that it has in the develop-

ment of the pharyngeal organs. These results also suggest that the redundant function that these genes have in affecting the migration of the pharyngeal organs may be due to their coexpression in the neural crest.

## CONCLUSIONS

We have used a genetic analysis of three paralogous *Hox* genes, *Hoxa3, Hoxb3,* and *Hoxd3,* to uncover a novel role for these genes in the morphogenesis of the pharyngeal organs. Our analysis showed that all three genes are important for proper migration of the thymus, ultimobranchial bodies, and parathyroids, but only *Hoxa3* seems to be required for thymus and parathyroid organogenesis.

Development of the pharyngeal organs normally occurs concurrent with their migration, during days E10.5 through E15.5 of development. The most severe defects seen in the multiple mutants correspond to events that normally occur around E12.5–E13.5 (see Fig. 1). The less severe ultimobranchial body phenotypes (persistent but not ectopic ultimobranchial body and partially, rather than fully, fused ultimobranchial body) correspond to a slightly later defect, at E13.5–E15.5. The migration of the organ primordia is unique to the pharyngeal organs, and the mechanism by which these cells migrate as a coherent group is not understood. However, since these tissues have a significant contribution from neural crest, it is tempting to suggest that mechanisms similar to those mediating migration of neural crest cells have been co-opted to allow the coherent migration of these very large groups of cells. Consistent with this hypothesis is the coexpression of *Hoxa3, Hoxb3,* and *Hoxd3* in the neural crest that contributes to the development of these organs. Loss of early expression of these genes in the migratory or postmigratory neural crest could result in defective organ development and migration. Because these phenotypes resemble a block in organ migration at the E12.5–E14.5 stage, this phenotype could also represent a later requirement for these genes. The expression patterns of these genes at later stages, and specifically in the pharyngeal organs, have not been examined in detail. Expression of both *Hoxa3* and *Hoxb3* have been reported in the developing thyroid primordia (Gaunt, 1988; Sham *et al.,* 1992), raising the possibility that expression of these genes is required later, during organ development.

Ectopic pharyngeal organs have also been reported in *RARα/γ* double-mutant mice (Mendelsohn *et al.,* 1994). This phenotype was interpreted as resulting from the effect of the RAR mutations on neural crest cell function. Since the retinoic acid signaling pathway is a potential activator of *Hox* gene expression during development (see Krumlauf, 1994, for review), the similarity between these phenotypes is consistent with the suggestion that the aberrant migration of pharyngeal organs in mice with multiple mutations in group 3 *Hox* genes is the result of the loss of expression of these three genes in the neural crest.

A possible explanation for the ectopic organs seen in these mutants is that there is a defect in cell migration. Several studies have shown that *Hox* genes play a role in cell migrations during development, particularly of neurons. In *C. elegans, mab5* and *lin39* are HOM C homologs that regulate cell migration of the Q daughter cells, which become sensory neurons (Salser and Kenyon, 1992, 1994; Harris *et al.,* 1996). Mutations in *mab5* and *lin39* affect both the direction and extent of migration of these cells during development. In mice, *Hox* genes are also expressed in migrating neurons. Independent mutations in *Hoxa1* and *Hoxb1* affect the migration of motor neurons within the hindbrain (Carpenter *et al.,* 1993; Mark *et al.,* 1993; Goddard *et al.,* 1996; Studer *et al.,* 1996). In *Hoxa1* mutant homozygotes, ectopic neurons that extend their axons to the seventh ganglion are found in rhombomeres 6, 7, and 8 and even in the rostral aspects of the spinal cord. Such neurons are never observed in normal mice. A reasonable hypothesis for the presence of these neurons at such caudal positions is hypermigrations of neurons normally restricted to rhombomeres 4 and 5. In the *Hoxb1* mutants, motor neurons that originate in rhombomere 4 and contribute to the facial motor nucleus fail to migrate, resulting in the absence of the seventh motor nucleus in these mutants.

The defect in thymus and parathyroid migration in the $Hoxa3^{+/-}$,$Hoxb3^{-/-}$,$Hoxd3^{-/-}$ mice combined with the apparently normal development of these ectopic organs shows that pharyngeal glandular organ development and migration during embryogenesis are genetically separable events. This result is consistent with the fact that in lower vertebrates, these organs do not migrate. The ultimobranchial body phenotype could also be considered to consist of two separate defects, the failure of the ultimobranchial body to interact with the thyroid lobes and a failure to migrate properly. Both the migration defect and failure to fuse are redundantly specified, although not to the degree seen in the thymus and parathyroids because the ultimobranchial body defects are seen in double mutants. It should also be noted that in chickens the ultimobranchial body does not fuse with the thyroid, remaining as a separate glandular organ. Thus, the changes in pharyngeal organ migration seen in these *Hox* mutants represent defects in morphological events that are unique to mammals.

The presence of follicles containing colloid in the ectopic ultimobranchial bodies suggests that some follicles may arise directly from the ultimobranchial bodies. The question of the embryological origins of the various cell populations within the thyroid gland has long been controversial. It is generally accepted that calcitonin-positive C cells originate in the ultimobranchial bodies and are of neural crest origin (Pearse and Carvalheira, 1967; Moseley *et al.,* 1968; Pearse and Polak, 1971; LeLievre and LeDouarin, 1975). However, a number of studies have suggested that both C cells and follicular cells have a dual origin, with both cell types being able to arise from both the thyroid diverticulum and the ultimobranchial body (Williams *et al.,* 1989; Harach, 1991; Conde *et al.,* 1992; Pueblitz *et al.,* 1993). Variation in ultimobranchial body and thyroid morphogenesis between species has contributed to the confusion on this issue (Rogers, 1927, and references therein). The apparent

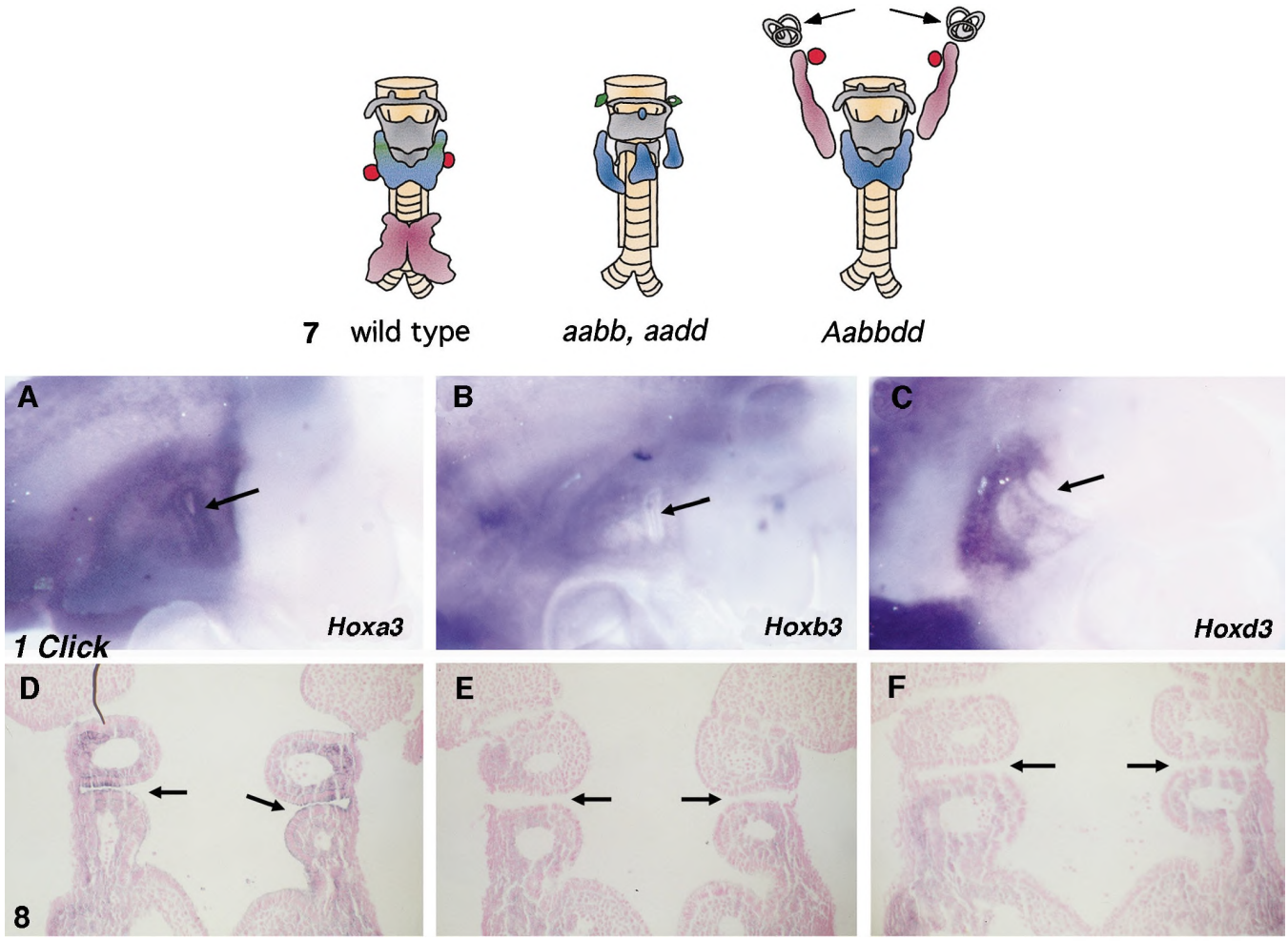


**FIG. 7.** The pharyngeal organ phenotypes in newborn multiple mutants. In the *Hoxa3*$^{-/-}$,*Hoxb3*$^{-/-}$ and *Hoxa3*$^{-/-}$,*Hoxd3*$^{-/-}$ double mutants, the ultimobranchial bodies are ectopically located above the thyroid, and the thyroid lobes are in pieces, or absent. Triangular pyramidal lobes are sometimes seen at the ventral midline, as are cervical thyroid tissue further cranially. The hyoid bone and the laryngeal cartilages are also deformed and reduced in size. The thymus and parathyroids are absent. In the *Hoxa3*$^{+/-}$,*Hoxb3*$^{-/-}$,*Hoxd3*$^{-/-}$ newborn animals, the thyroid lobes appear essentially normal. Because the ultimobranchial body phenotype was not conclusively determined (see Results), they are not shown for this genotype. The thymus lobes are lateral and anterior to the thyroid. The parathyroids are associated with the thymus lobes medial to their anterior ends, which are located near the inner ear (arrows).

**FIG. 8.** Expression pattern of the group 3 paralogs at E10.5 in the pharyngeal arches and pouches. A and D have been previously published (Manley and Capecchi, 1995) and are included here for comparison. (A–C) Lateral views of the pharyngeal arch region of E10.5 wild-type embryos stained by whole-mount *in situ* for each of the group 3 paralogs. Dorsal is up, cranial is to the right. The arrow points to the third pharyngeal pouch in each panel. *Hoxa3* is strongly expressed in the third pouch, while *Hoxb3* and *Hoxd3* are not. (D–F) E10.5 embryos first processed by whole-mount *in situ* and then embedded in paraffin, sectioned in the coronal plane, and counterstained with nuclear Fast Red. Cranial is up. Arrows point to the third pharyngeal pouches in each panel. Although all three genes are expressed in the arch mesenchyme, particularly in arch 4 (below the arrows), only *Hoxa3* is expressed in the endodermal cells of the third pharyngeal pouch.

presence of colloid-containing follicles in some of the persistent ultimobranchial bodies in the double mutants is consistent with thyroglobulin-producing follicular cells having such a dual origin. Interestingly, in the Echidna ultimobranchial bodies never fuse with the thyroid gland, and also have colloid-containing follicles (Maurer, 1899). However, the consistent lack of calcitonin-positive cells in the thyroid in the absence of ultimobranchial body fusion strongly suggests that the ultimobranchial body is the only source of C cells, at least in the mouse.

Both the thyroid diverticulum and the ultimobranchial body may be separately affected by these mutations. All three paralogs have a role in ultimobranchial body development as revealed in the double mutants. While the increase in severity of the ultimobranchial body defects in the double mutants is clear, the effect on the follicular lobes of the thyroid is less dramatic. The presence of pyramidal lobes and the broken thyroid lobe structure may represent an increase in the severity of defects in the organization or migratory behavior of thyroid diverticulum-derived tissue.

Pyramidal lobes and cervical thyroid tissue are thought to be remnants of the medial migration path of the thyroid. However, it is possible that any apparent exacerbation of the $Hoxa3^{-/-}$ phenotype in the structure of the thyroid lobes could be secondary to the increased severity of the ultimobranchial body defects in the double mutants. While double mutants with *Hoxa3* may have a slight increase in the severity of defects in thyroid lobe structure, the follicular cells themselves do not seem to be more severely affected. Also, the $Hoxb3^{-/-}$,$Hoxd3^{-/-}$ double mutant and the $Hoxa3^{+/-}$, $Hoxb3^{-/-}$,$Hoxd3^{-/-}$ mutants do not seem to have any defects in the follicular lobes or the isthmus. These results suggest that the *Hox* group 3 paralogs may not play a significant direct role in the development of the thyroid diverticulum, and that the interaction between the thyroid diverticulum and the ultimobranchial body is critical for the proper development of the thyroid gland. A reason that the thyroid diverticulum may not be directly under the influence of these *Hox* genes is that its site of origin (Fig. 1) is not within the pharyngeal pouches. Alternatively, the thyroid lobe defects could be secondary to changes in extracellular matrix, or in cell adhesion properties along the migratory route, independent of ultimobranchial body defects.

Thymus and parathyroid organ development, on the other hand, is extremely dependent on *Hoxa3* function. One possible explanation for this apparently unique function for *Hoxa3* may be found in the comparison of the expression patterns of the group 3 paralogs. At E10.5, when development of these glandular organs is beginning, only *Hoxa3* is expressed in the third pharyngeal pouch endoderm cells. Transplantation studies in the chick have shown that the endoderm has a primary role in specifying thymus development (LeDouarin and Jotereau, 1975). The importance of interactions between pouch endoderm and neural crest cells has also been demonstrated (Auerbach, 1960; Bockman and Kirby, 1984; Anderson *et al.,* 1993). The fact that *Hoxa3,* alone in this paralogous group, is expressed in the pouch endoderm may explain its singular role in the development of the thymus and parathyroids.

In summary, we have shown that among the group 3 paralogous genes, *Hoxa3* is the principal player required for forming the pharyngeal organs. In the absence of *Hoxa3* function, the thymus and parathyroids are not formed. However, in combination with the *Hoxa3* mutation, addition of mutations in *Hoxb3* or *Hoxd3* exacerbates the impact on pharyngeal organ development, with increased frequency and severity of defects being seen in formation, subsequent migratory pattern and fusion of the ultimobranchial body with the thyroid. Finally, mice heterozygous for the *Hoxa3* loss-of-function mutations and homozygous for the *Hoxb3* and *Hoxd3* mutations show defects in the migratory pattern of the thymus and parathyroid glands. This observation suggests a highly redundant role for all three of these *Hox* genes in regulating the migration of these very large groups of cells.

## REFERENCES

Anderson, G., Jenkinson, E. J., Moore, N. C., and Owen, J. J. T. (1993). MHC class II-positive epithelium and mesenchyme are both required for T-cell development in the thymus. *Nature* **362,** 70–73.

Auerbach, R. (1960). Morphogenetic interactions in the development of the mouse thymus gland. *Dev. Biol.* **2,** 271–284.

Barrow, J., and Capecchi, M. R. (1996). Targeted disruption of the *Hoxb-2* locus in mice interferes with expression of *Hoxb-1* and *Hoxb-4*. *Development* **122,** 3817–3828.

Behringer, R. R., Crotty, D. A., Tennyson, V. M., Brinster, R. L., Palmiter, R. D., and Wolgemuth, D. J. (1993). Sequences 5′ of the homeobox of the *Hox-1.4* gene direct tissue-specific expression of *lacZ* during mouse development. *Development* **117,** 823–833.

Benson, G., Lim, H., Paria, B., Satokata, I., Dey, S. and Maas, R. (1996). Mechanisms of reduced fertility in Hoxa-10 mutant mice: uterine homeosis and loss of maternal Hoxa-10 expression. *Development* **122,** 2687–2696.

Bockman, D. E., and Kirby, M. L. (1984). Dependence of thymus development on derivatives of the neural crest. *Science* **223,** 498–500.

Bogarad, L. D., Utset, M. F., Awgulewitsch, A., Miki, T., Hart, C. P., and Ruddle, F. H. (1989). The developmental expression pattern of a new murine homeo box gene: Hox-2.5. *Dev. Biol.* **133,** 537–549.

Boulet, A. M., and Capecchi, M. R. (1996). Targeted disruption of *hoxc-4* causes esophageal defects and vertebral transformations. *Dev. Biol.* **177,** 232–249.

Carpenter, E. M., Goddard, J. M., Chisaka, O., Manley, N. R., and Capecchi, M. R. (1993). Loss of *Hox-A1 (Hox-1.6)* function results in the reorganization of the murine hindbrain. *Development* **118,** 1063–1075.

Chisaka, O., and Capecchi, M. R. (1991). Regionally restricted developmental defects resulting from targeted disruption of the mouse homeobox gene *hox-1.5*. *Nature* **350,** 473–479.

Chisaka, O., Musci, T. S., and Capecchi, M. R. (1992). Developmental defects of the ear, cranial nerves and hindbrain resulting from targeted disruption of the mouse homeobox gene *Hox-1.6*. *Nature* **355,** 516–520.

Conde, E., Moreno, A. M., Martin-Lacave, I., Fernandez, A. and Galera, H. (1992). Immunocytochemical study of the ultimobranchial tubule in Wistar rats. *Anat. Histol. Embryol.* **21,** 94–100.

Condie, B. G., and Capecchi, M. R. (1993). Mice homozygous for a targeted disruption of *Hoxd-3 (Hox-4.1)* exhibit anterior transformations of the first and second cervical vertebrae, the atlas and the axis. *Development* **119,** 579–595.

Condie, B. G., and Capecchi, M. R. (1994). Mice with targeted disruptions in the paralogous genes *hoxa-3* and *hoxd-3* reveal synergistic interactions. *Nature* **370,** 304–307.

Cordier, A. C., and Haumont, S. M. (1980). Development of thymus, parathyroids, and ultimobranchial bodies in NMRI and Nude mice. *Am. J. Anat.* **157,** 227–263.

Davis, A. P., and Capecchi, M. R. (1994). Axial homeosis and appendicular skeleton defects in mice with a targeted disruption of *hoxd-11*. *Development* **120,** 2187–2198.

Davis, A. P., Witte, D. P., Hsieh-Li, H. M., Potter, S. S., and Capecchi, M. R. (1995). Absence of radius and ulna in mice lacking *hoxa-11* and *hoxd-11*. *Nature* **375,** 791–795.

Davis, A. P., and Capecchi, M. R. (1996). A mutational analysis of the 5′ Hox D genes: Dissection of genetic interactions during limb development in the mouse. *Development* **122,** 1175–1185.

Dollé, P., Izpisúa-Belmonte, J.-C., Brown, J. M., Tickle, C. and Duboule, D. (1991). *Hox-4* genes and the morphogenesis of mammalian genitalia. *Genes Dev.* **5,** 1767–1776.

Dollé, P., Dierich, A., LeMeur, M., Schimmang, T., Schuhbaur, B.,

Chambon, P., and Duboule, D. (1993). Disruption of the *Hoxd-13* gene induces localized heterochrony leading to mice with neotenic limbs. *Cell* **75,** 431–441.

Dony, C., and Gruss, P. (1987). Specific expression of the *Hox-1.3* homeo box gene in murine embryonic structures originating from or induced by the mesoderm. *EMBO J.* **6,** 2965–2975.

Fibi, M., Zink, B., Kessel, M., Colberg-Poley, A. M., Labeit, S., Lehrach, H., and Gruss, P. (1988). Coding sequence and expression of the homeobox gene *Hox 1.3*. *Development* **102,** 349–359.

Frohman, M. A., Boyle, M., and Martin, G. R. (1990). Isolation of the mouse *Hox-2.9* gene; analysis of embryonic expression suggests that positional information along the anterior–posterior axis is specified by mesoderm. *Development* **110,** 589–607.

Fromental-Ramain, C., Warot, X., Lakkaraju, S., Favier, B., Haack, H., Birling, C., Dierich, A., Dollé, P., and Chambon, P. (1996a). Specific and redundant functions of the paralogous *Hoxa-9* and *Hoxd-9* genes in forelimb and axial skeleton patterning. *Development* **122,** 461–472.

Fromental-Ramain, C., Warot, X., Messadecq, N., LeMeur, M., Dolle, P., and Chambon, P. (1996b). *Hoxa-13* and *hoxd-13* play a crucial role in the patterning of the limb autopod. *Development* **122,** 2997–3011.

Gamer, L. W., and Wright, C. V. E. (1993). Murine *Cdx-4* bears striking similarities to the *Drosophila caudal* gene in its homeodomain sequence and early expression pattern. *Mech. Dev.* **43,** 71–81.

Gaunt, S. J. (1987). Homeobox gene *Hox1.5* expression in mouse embryos: earliest detection by *in situ* hybridization is during gastrulation. *Development* **101,** 51–60.

Gaunt, S. J. (1988). Mouse homeobox gene transcripts occupy different but overlapping domains in embryonic germ layers and organs: a comparison of *Hox-3.1* and *Hox-1.5*. *Development* **103,** 135–144.

Gaunt, S. J., Krumlauf, R., and Duboule, D. (1989). Mouse homeogenes within a subfamily, *Hox-1.4, -2.6* and *-5.1* display similar anteroposterior domains of expression in the embryo, but show stage- and tissue-dependent differences in their regulation. *Development* **107,** 131–141.

Gaunt, S. J., Coletta, P. L., Pravtcheva, D., and Sharpe, P. T. (1990). Mouse Hox-3.4: homeobox sequence and embryonic expression patterns compared with other members of the Hox gene network. *Development* **109,** 329–339.

Geada, A. M., Gaunt, S. J., Azzawi, M., Shimeld, S. M., Pearce, J., and Sharpe, P. T. (1992). Sequence and embryonic expression of the murine *Hox-3.5* gene. *Development* **116,** 497–506.

Gendron-Maguire, M., Mallo, M., Zhang, M., and Gridley, T. (1993). *Hoxa-2* mutant mice exhibit homeotic transformation of skeletal elements derived from cranial neural crest. *Cell* **75,** 1317–1331.

Goddard, J. M., Rossel, M., Manley, N. R., and Capecchi, M. R. (1996). Mice with targeted disruption of *Hoxb-1* fail to form the motor nucleus of the VIIth nerve. *Development* **122,** 3217–3228.

Goto, J., Miyabayashi, T., Wakamatsu, Y., Takahashi, N., and Muramatsu, M. (1993). Organization and expression of mouse *Hox 3* cluster genes. *Mol. Gen. Genet.* **239,** 41–48.

Haack, H., and Gruss, P. (1993). The establishment of murine *Hox-1* expression domains during patterning of the limb. *Dev. Biol.* **157,** 410–422.

Harach, H. R. (1991). Thyroglobulin in human thyroid follicles with acid mucin. *J. Pathol.* **164,** 261–263.

Harris, J., Honigberg, L., Robinson, N., and Kenyon, C. (1996). Neuronal cell migration in *C. elegans:* regulation of Hox gene expression and cell position. *Development* **122,** 3117–3131.

Hilfer, S. R. (1968). Cellular interactions in the genesis and maintenance of thyroid characteristics. *In* "Epithelial–Mesenchymal Interactions" (R. Fleischmajer and R. E. Billingham, Eds.), pp. 177–199. Williams and Wilkins, Baltimore.

Holland, P. W. H., and Hogan, B. L. M. (1988). Spatially restricted pattern of expression of the homeobox-containing gene, *Hox-2.1* during mouse embryogenesis. *Development* **102,** 159–174.

Hunt, P., Gulisano, M., Cook, M., Sham, M.-H., Faiella, A., Wilkinson, D., Boncinelli, E., and Krumlauf, R. (1991a). A distinct *Hox* code for the branchial region of the vertebrate head. *Nature* **353,** 861–864.

Hunt, P., Whiting, J., Nonchev, S., Sham, M.-H., Marshall, H., Graham, A., Cook, M., Allemann, R., Rigby, P. W. J., Gulisano, M., Faiella, A., Boncinelli, E., and Krumlauf, R. (1991b). The branchial *Hox* code and its implications for gene regulation, patterning of the nervous system and head evolution. *Dev. Suppl.* **2,** 63–77.

Jeannotte, L., Lemieux, M., Charron, J., Poirier, F., and Robertson, E. J. (1993). Specification of axial identity in the mouse: role of the *Hoxa-5* (*Hox-1.3*) gene. *Genes Dev.* **7,** 2085–2096.

Kalter, H., and Warkaney, J. (1961). Experimental production of congenital malformations in strains of inbred mice by maternal treatment with hypervitaminosis A. *Am. J. Pathol.* **38,** 1–21.

Kostic, D., and Capecchi, M. R. (1994). Targeted disruptions of the murine *hoxa-4* and *hoxa-6* genes result in homeotic transformations of components of the vertebral column. *Mech. Dev.* **46,** 231–247.

Kress, C., Vogels, R., Graaff, W. D., Bonnerot, C., Meijlink, F., Nicolas, J. F., and Deschamps, J. (1990). *Hox-2.3* upstream sequences mediate *lacZ* expression in intermediate mesoderm derivations of transgenic mice. *Development* **109,** 775–786.

Krumlauf, R., Holland, P. W., McVey, J. H., and Hogan, B. L. M. (1987). Developmental and spatial patterns of expression in the mouse homeobox gene *Hox 2.1*. *Development* **99,** 603–617.

LeDouarin, N., and Jotereau, F. V. (1975). Tracing of cells or the avian thymus through embryonic life in interspecific chimeras. *J. Ex. Med.* **142,** 17–40.

LeLievre, C. S., and LeDouarin, N. M. (1975). Mesenchymal derivatives of the neural crest: analysis of chimaeric quail and chick embryos. *J. Embryol. Exp. Morphol.* **34,** 125–154.

LeMouellic, H., Lallemand, Y., and Brûlet, P. (1992). Homeosis in the mouse induced by a null mutation in the *Hox-3.1* gene. *Cell* **69,** 251–264.

Manley, N. R., and Capecchi, M. R. (1995). The role of *hoxa-3* in mouse thymus and thyroid development. *Development* **121,** 1989–2003.

Manley, N. R., and Capecchi, M. R. (1997). Hox group 3 paralogous genes act synergistically in the formation of somitic and neural crest-derived structures. *Dev. Biol.* **192,** 274–288.

Mansour, S. L., Goddard, J. M., and Capecchi, M. R. (1993). Mice homozygous for a targeted disruption of the proto-oncogene *int-2* have developmental defects in the tail and inner ear. *Development* **117,** 13–28.

Mark, M., Lufkin, T., Vonesch, J.-L., Ruberte, E., Olivo, J.-C., Dollé, P., Gorry, P., Lumsden, A., and Chambon, P. (1993). Two rhombomeres are altered in *Hoxa-1* mutant mice. *Development* **119,** 319–338.

Maurer, F. (1899). Die Schlundspalten-derivate von Echidna. *Anat Anz. Erganzungshefte zu bd.* **16,** S. 88–101.

Mendelsohn, C., Lohnes, D., Decimo, D., Lufkin, T., LeMeur, M., Chambon, P., and Mark, M. (1994). Function of the retinoic acid receptors (RARs) during development: (II) Multiple abnormalities at various stages of organogenesis in RAR double mutants. *Development* **120,** 2749–2771.

Moseley, J. M., Mathews, E. W., Breed, R. H., Galante, L., Tse, A., and MacIntyre, I. (1968). The ultimobranchial origin of calcitonin. *Lancet* **1,** 108–110.

Pearse, A. G. E., and Carvalheira, A. F. (1967). Cytochemical evidence for an ultimobranchial origin of rodent thyroid C cells. *Nature* **214,** 929–930.

Pearse, A. G. E., and Polak, J. M. (1971). Cytochemical evidence for the neural crest origin of mammalian ultimobranchial C cells. *Histochemie* **27,** 96–102.

Peterson, R. L., Papenbrock, T., Davda, M. M., and Awgulewitsch, A. (1994). The murine *Hoxc* cluster contains five neighboring *AbdB*-related Hox genes that show unique spatially coordinated expression in posterior embryonic subregions. *Mech. Dev.* **47,** 253–260.

Pueblitz, S., Weinberg, A. G., and Albores-Saavedra, J. (1993). Thyroid C cells in the DiGeorge anomaly: a quantitative study. *Pediatr. Pathol.* **13,** 463–473.

Ramirez-Solis, R., Zheng, H., Whiting, J., Krumlauf, R., and Bradley, A. (1993). *Hoxb-4* (*Hox-2.6*) mutant mice show homeotic transformation of a cervical vertebra and defects in the closure of the sternal rudiments. *Cell* **73,** 279–294.

Rijli, F. M., Mark, M., Lakkaraju, S., Dierich, A., Dollé, P., and Chambon, P. (1993). A homeotic transformation is generated in the rostral branchial region of the head by disruption of *Hoxa-2,* which acts as a selector gene. *Cell* **75,** 1333–1349.

Rijli, F., Matyas, R., Pelligrini, M., Dierich, A., Gruss, P., Dolle, P., and Chambon, P. (1995). Cryptorcidism and homeotic transformations of spinal nerves and vertebrae in Hoxa-10 mutant mice. *Proc. Natl. Acad. Sci. USA* **92,** 8185–8189.

Rogers, W. M. (1927). The fate of the ultimobranchial body in the white rat (*Mus norvegicus albinus*). *Am. J. Anat.* **38,** 349–477.

Rogers, W. M. (1971). Normal and anomalous development of the thyroid. *In* "The Thyroid" (S. C. Werner and S. H. Ingbar, Ed.), pp. 303–317. Harper and Row, New York.

Salser, S. J., and Kenyon, C. (1992). Activation of a *C. elegans Antennapedia* homologue in migrating cells controls their direction of migration. *Nature* **355,** 255–258.

Salser, S. J., and Kenyon, C. (1994). Patterning *C. elegans:* homeotic cluster genes, cell fates, and cell migrations. *Trends Genet.* **10,** 159–164.

Satokata, I., Benson, G., and Maas, R. (1995). Sexually dimorphic sterility phenotypes in *Hoxa10*-deficient mice. *Nature* **374,** 460–463.

Schughart, K., Utset, M. F., Awgulewitsch, A., and Ruddle, F. H. (1988). Structure and expression of Hox-2.2, a murine homeobox-containing gene. *Proc. Natl. Acad. Sci. USA* **85,** 5582–5586.

Sham, M. H., Hunt, P., Nonchev, S., Papalopulu, N., Graham, A., Boncinelli, E., and Krumlauf, R. (1992). Analysis of the murine *Hox-2.7* gene: conserved alternative transcripts with differential distributions in the nervous system and the potential for shared regulatory regions. *EMBO J.* **11,** 1825–1836.

Small, K. M., and Potter, S. S. (1993). Homeotic transformations and limb defects in *HoxA-11* mutant mice. *Genes Dev.* **7,** 2318–2328.

Studer, M., Lumsden, A., Ariza-McNaughton, L., Bradley, A., and Krumlauf, R. (1996). Altered segment identity and abnormal migration of motor neurons in mice lacking Hoxb-1. *Nature* **384,** 630–634.

Suemori, W., Takahashi, N., and Noguchi, S. (1995). *Hoxc-9* mutant mice show anterior transformation of the vertebrae and malformation of the sternum and ribs. *Mech. Dev.* **51,** 265–273.

Tan, D.-P., Ferrante, J., Nazarali, A., Shao, X., Kozak, C. A., Guo, V., and Nirenberg, M. (1992). Murine *Hox-1.11* homeobox gene structure and expression. *Proc. Natl. Acad. Sci. USA* **89,** 6280–6284.

Wall, N. A., Jones, C. M., Hogan, B. L. M., and Wright, C. V. E. (1992). Expression and modification of *hox-2.1* protein in mouse embryos. *Mech. Dev.* **37,** 111–120.

Whiting, J., Marshall, H., Cook, M., Krumlauf, R., Rigby, P. W., Stott, D., and Allemann, R. K. (1991). Multiple spatially specific enhancers are required to reconstruct the pattern of *Hox-2.6* gene expression. *Genes Dev.* **5,** 2048–2059.

Williams, E. D., Toyn, C. E., and Harach, H. R. (1989). The ultimobranchial gland and congenital thyroid abnormalities in man. *J. Pathol.* **159,** 135–141.

Zákány, J., and Duboule, D. (1996). Synpolydactyly in mice with a targeted deficiency in the *HoxD* complex. *Nature* **384,** 69–71.

Received for publication October 15, 1997
Accepted December 8, 1997